mater.scichina.com link.springer.com

Published online 21 January 2021 | https://doi.org/10.1007/s40843-020-1550-2
Sci China Mater 2021, 64(6): 1386–1395

Realizing excellent cycle stability of Zn/$Na_3V_2(PO_4)_3$ batteries by suppressing dissolution and structural degradation in non-aqueous Na/Zn dual-salt electrolytes

Qian Li[1], Kaixuan Ma[1], Cheng Hong[1], Gongzheng Yang[1*] and Chengxin Wang[1,2*]

ABSTRACT **The low-cost and high-safety rechargeable zinc-ion batteries (ZIBs) show promising applications for large-scale energy storage. However, the (de)intercalation of divalent zinc ions with high charge density restricts cathode materials' choice. $Na_3V_2(PO_4)_3$ (NVP) is one of the sodium (Na) super-ionic conductor materials that shows feasible utilization in aqueous ZIBs but universally has poor cycle life, commonly limited to 200 cycles or less. In this study, we investigate the capacity degradation mechanism of NVP systematically and then propose a novel organic dual-salt electrolyte to realize excellent cycling stability. We find a spontaneous dissolution of NVP when immersed in the static aqueous electrolyte, and there is an irreversible phase change during the first discharge process, leading to a fast capacity fading in aqueous electrolytes. The dissolution problem can be effectively suppressed by non-aqueous Zn^{2+}-containing electrolytes. However, the sluggish reaction of Zn^{2+} intercalation into NVP causes poor reversibility. We develop a non-aqueous Na/Zn hybrid system by adding Na^+ ions as charge carriers to address this issue. Highly reversible co-insertion of Na/Zn ions into the NVP enables a high capacity of 84 mA h $^{-1}$ and an outstanding lifetime of 600 cycles at 500 mA g^{-1} without capacity loss. This work provides valuable views on the NVP's failure mechanisms that will be helpful for ZIB development.**

Keywords: energy storage, Zn battery, $Na_3V_2(PO_4)_3$, Na/Zn dual-salt electrolyte, long life

INTRODUCTION

Demands for large-scale energy storage cannot be met with lithium-ion batteries because of the risks of flammable electrolytes and the rare reserves of lithium sources. Thus, there is an urgency for non-toxic, environmentally friendly, and cheap energy storage devices [1–3]. Recently, researchers made increasing concerns on the multivalent-ion (Zn^{2+}, Ca^{2+}, and Mg^{2+}) batteries that directly use metallic anode [4–7]. Zinc metal is an ideal negative electrode because of its reasonable redox potential (−0.763 V *vs.* standard hydrogen electrode), low cost, high safety, and high volumetric capacity density of 5855 mA h cm^{-3} [8,9]. Considering these zinc merits, we found that zinc-ion batteries (ZIBs) show good advantages in large-scale energy storage. However, there are many challenges with applying ZIBs, such as the lack of cathode materials with long cycle life [10–14]. Compared with alkali metal ions, divalent zinc ions' high charge density brings stronger electrostatic interactions with positive materials, leading to many limitations in exploiting suitable cathode materials [9,15,16]. For improving the electrochemical performance of ZIBs, it is significant to develop a feasible material with a stable structure.

$Na_3V_2(PO_4)_3$ (NVP) is one of the sodium (Na) super-ionic conductor (NASICON) materials that are commonly applied as cathode materials in Na-ion batteries with impressively long cycle life [17–20]. The stable three-dimensional (3D) framework structure of NVP is favorable for long cycle life, providing possible applications to store zinc ions, which have smaller radii (0.72 Å) than Na^+ ions (1.02 Å) [21]. Li *et al.* [22] successfully attempted the NVP electrode in ZIBs, in which NVP exhibited a working voltage of 1.1 V and a high specific

[1] State Key Laboratory of Optoelectronic Materials and Technologies, School of Materials Science and Engineering, Sun Yat-sen University, Guangzhou 510275, China
[2] The Key Laboratory of Low-carbon Chemistry & Energy Conservation of Guangdong Province, Sun Yat-sen University, Guangzhou 510275, China
* Corresponding authors (emails: yanggzh5@mail.sysu.edu.cn (Yang G); wchengx@mail.sysu.edu.cn (Wang C))

capacity of 97 mA h g^{-1}. Subsequently, Li *et al.* [23] employed a Na^+- and Zn^{2+}-containing aqueous electrolyte and improved the conductivity of NVP by wrapping with graphene-like carbon. During cycling in the hybrid system, the insertion and extraction of Na^+ ions in the structure deliver a capacity of 92 mA h g^{-1}; however, the battery demonstrated an unsatisfactory cycle life (200 cycles). Mai and co-workers [24] reported another hybrid electrolyte and demonstrated the simultaneous insertion of Na^+ and Zn^{2+} ions in NVP; however, the lifespan remained only 200 cycles. To explain the capacity fading mechanism of NVP, Zhang *et al.* [25] proposed that the transition of high crystallinity to nanocrystalline during cycling may result in severe capacity fading. Therefore, relevant research regarding NVP in ZIBs is still in an infancy state. The capacity attenuation mechanisms and corresponding solution methods need to be further studied.

In this study, we used an NVP@C cathode in a non-aqueous Na/Zn hybrid-ion battery. We investigated the cathode materials' capacity fading mechanisms in both aqueous and non-aqueous ZIBs, unveiling that the charging process will further promote the spontaneous dissolution of NVP in aqueous electrolytes. During the discharge process, a large amount of $Zn_3(PO_4)_2$ and $VOPO_4$ simultaneously formed on the electrodes' surface, making it hard for NVP to achieve good cycling performance in an aqueous environment. We then developed a non-aqueous Zn^{2+}-containing electrolyte. Unfortunately, it is challenging for the sluggishly intercalated Zn^{2+} ions to extract from NVP, causing structural degradation and poor cycling performance. By introducing Na^+ ions into the non-aqueous electrolyte, we found that the Na/Zn dual salt is conducive to eliminating the NVP dissolution and beneficial for highly reversible cation insertion and removal. Hence, the NVP@C electrodes demonstrate good electrochemical performances: high capacity of 84 mA h g^{-1}, high average working voltage of 1.3 V, and long-term cycling capability (600 cycles with 100% capacity retention). We believed that this work could serve as a reference and guidance for the research of NVP in ZIBs.

EXPERIMENTAL SECTION

NVP@C preparation

To synthesize the NVP@C, we performed a simple one-step annealing method. Typically, 10 mmol vanadyl acetylacetonate was added into 30 mL *N*,*N*-dimethylformamide (DMF) to form solution A. NaH_2PO_4 (15 mmol) and glucose (1 g) were dissolved in 30 mL deionized water to form solution B. Solutions A and B were mixed homogenously and then evaporated to dryness to get a green composite. The product was obtained by annealing in a 5% H_2/Ar atmosphere at 700 °C for 6 h.

Characterizations

Using Cu Kα radiation at a voltage of 40 kV, we collected the X-ray diffraction (XRD) patterns on an X-ray diffractometer (Rigaku Co., Japan). We collected the transmission electron microscopy (TEM), high-resolution TEM (HRTEM), and elemental mapping images *via* TEM (FEI Tecnai G2 F30, 300 kV, USA) with an accelerating voltage of 300 kV. We performed the scanning electron microscopy (SEM) and energy-dispersive spectroscopy (EDS) tests *via* SEM (JSM-7001F, JEOL, 15 kV, France); micrographs were recorded at 15 kV. We obtained the XPS spectra using PerkinElmer PHI 1600 ESCA spectrometer (Waltham, USA).

Electrochemical test

The CR2032 coin-type batteries were manufactured with zinc metal anode, different electrolytes, and NVP@C cathode to test the electrochemical performance of NVP@C. In this study, the aqueous electrolyte was a mixed solution of 1 mol L^{-1} $NaCF_3SO_3$ and 0.1 mol L^{-1} $Zn(CF_3SO_3)_2$. A mixed solution of 1 mol L^{-1} $NaCF_3SO_4$ and 0.1 mol L^{-1} $Zn(CF_3SO_3)_2$ in triethyl phosphate (TEP) was used as the Na/Zn dual-salt electrolyte. $Zn(CF_3SO_3)_2$ (0.1 mol L^{-1}) in TEP was used as a pure Zn^{2+}-containing electrolyte. The separator was a glass fiber (GF/A, Whatman, Maidstone, Kent, UK). To get the NVP@C electrodes, we mixed the slurry of NVP@C, acetylene black, and polyvinylidene fluoride (PVDF) at a weight ratio of 7:2:1 in the polyvinylidene fluoride (NMP) solvent. The homogeneous mixture was cast on a graphite paper and then dried at 80°C overnight. The mass loading of active materials was 1.0–2.0 mg cm^{-2}. The cycling performances were tested using a battery tester (NEWARE, Shenzhen, China). Cyclic voltammetry (CV) tests were performed on an electrochemistry workstation (CHI660; CH Instruments Inc., Shanghai, China).

RESULTS AND DISCUSSION

The NVP was synthesized through a simple annealing process. Fig. 1a displays the XRD patterns of the obtained NVP, which matches well with the NVP's rhombohedral phase (JCPDS no. 53-0018) and depicts the corresponding crystal structure along the *a*-axis. As illustrated, the 3D framework of NVP is built by corner-shared PO_4

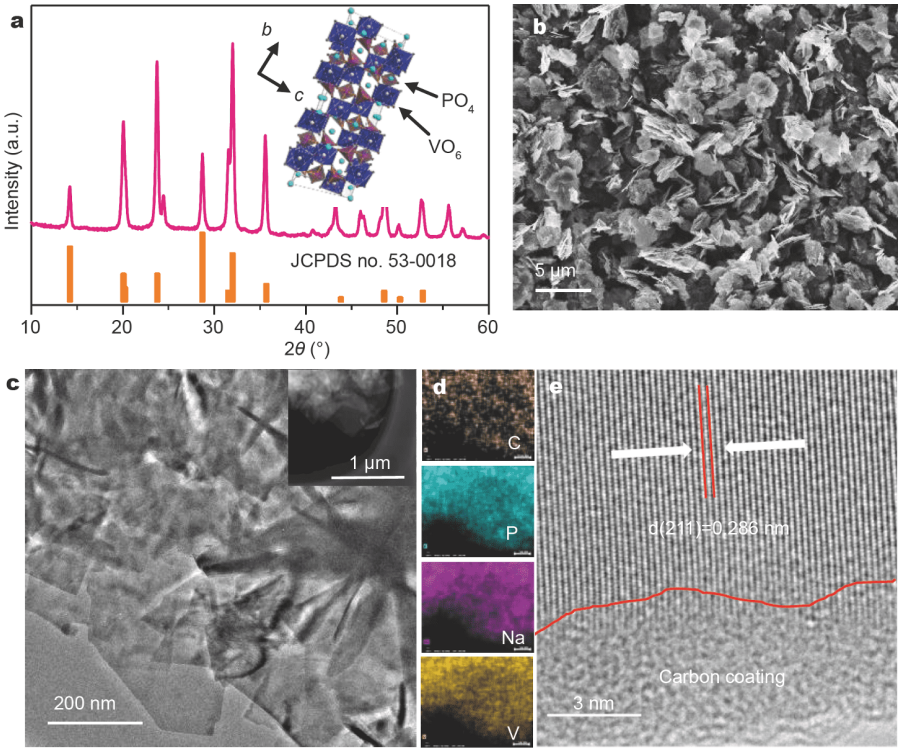

Figure 1 Crystal information and electron microscopy characterization of NVP. (a) XRD pattern and the schematic crystal structure along the *a*-axis of NVP. (b) SEM, (c) TEM, (d) elemental mapping, and (e) HRTEM images of NVP.

tetrahedral and VO_6 octahedral, in which two Na^+ ions can be extracted during charging [26,27]. SEM and TEM characterizations reveal the nanoflake-like morphology of NVP, as shown in Fig. 1b, c, respectively. Homogeneous distribution of C, Na, P, and V elements is evidenced by the scanning TEM and elemental mapping images in Fig. 1c, d, respectively. HRTEM image in Fig. 1e displays a carbon coating layer on the surface of NVP. The marked lattice fringe with a spacing distance of 0.286 nm belongs to the (211) plane. Benefiting from carbon coating, we found that the good electronic and ionic conductivity of NVP are favorable to high-rate performance [28].

The electrochemical performance can be improved by considering the mixed intercalation of Na^+ and Zn^{2+} ions in NVP [29]. To realize non-aqueous Zn/NVP batteries, we proposed a non-aqueous Na/Zn dual-salt electrolyte. To verify its feasibility, we combined the *ex-situ* XRD, XPS, and elemental mapping analyses for studying the reaction mechanisms of NVP. XRD patterns at selected 2θ regions of the first two cycles and the corresponding contour map are illustrated in Fig. S1 and Fig. 2a, respectively. A set of new peaks emerge during charging and disappear during discharging. The new phase can be denoted as $NaV_2(PO_4)_3$ because two Na ions can be extracted from NVP, as discussed in the literatures [22,30]. Simultaneously, the peaks belonging to NVP vanish at charging and reappear upon discharging. In aqueous electrolytes, the co-intercalation reaction of Na^+ and Zn^{2+} ions into NVP was previously reported. We presumed that the Zn^{2+} ions could also be co-inserted into NVP when employing a non-aqueous Na/Zn hybrid electrolyte.

A weak Zn signal at a discharged state was observed in EDS, as shown in Fig. S2. The elemental mapping in Fig. 2b depicted the homogenous distribution of Na and Zn elements, verifying the co-insertion mechanism. Thus, the formula of cathode materials at the discharged state can be assigned as $Zn_xNa_yV_2(PO_4)_3$. XPS characterizations were performed to examine the valence states and surface composite changes of NVP. Fig. 2c, d display the Na 1s and Zn 2p regions, respectively. Na peaks' intensity decreases at the charged state and intensifies after being fully discharged, indicating incomplete extraction of Na ions. Besides, the strong signals of Zn 2p can be detected at a discharged state, matching well with the EDS result. During cycling, the reversible chemical valence changes of V are evidenced in the V 2p region. As shown in Fig. 2e, the charged electrodes exhibit both V^{3+} ($2p_{3/2}$:

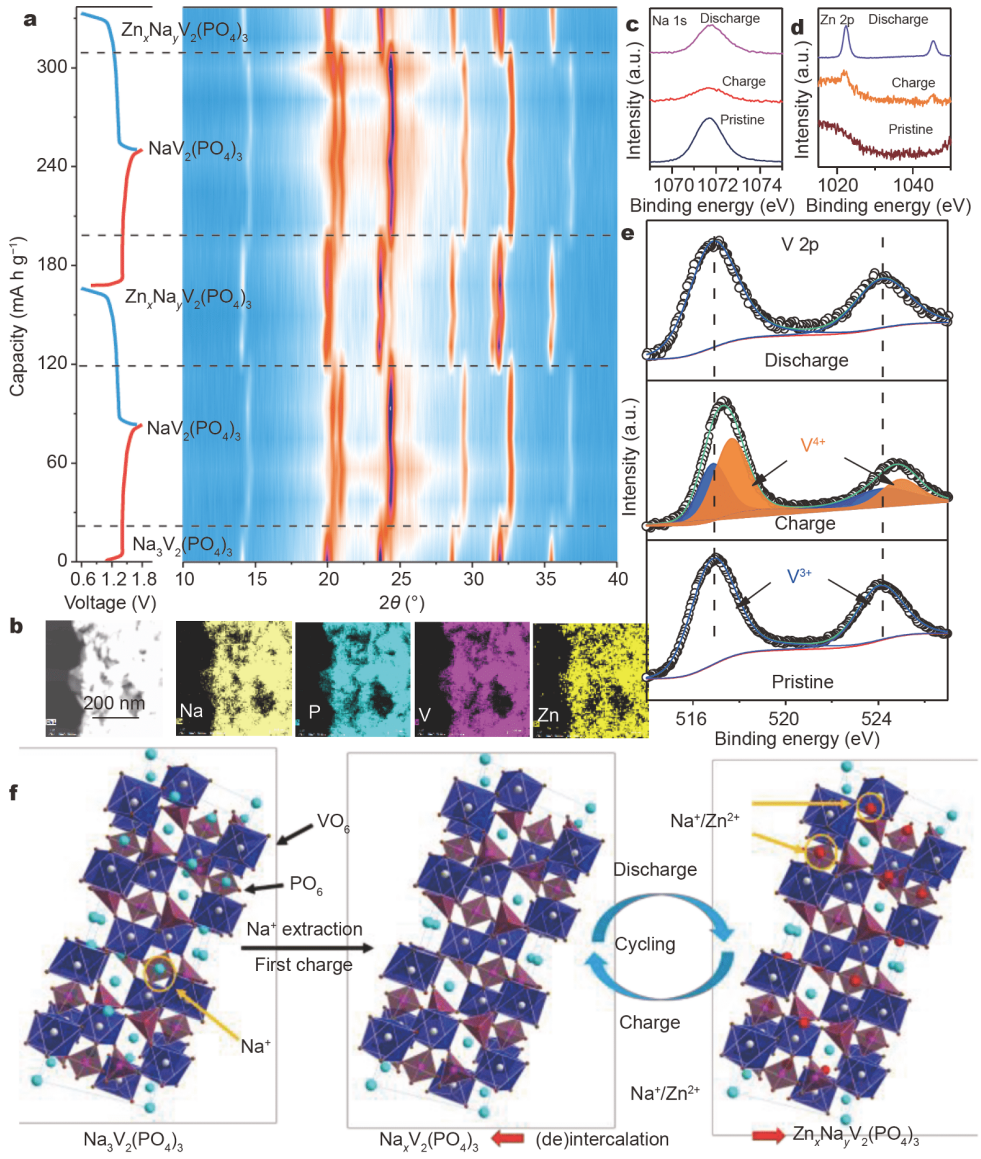

Figure 2 The reaction mechanism of NVP. (a) The *ex-situ* XRD contour map in the selected region for NVP electrodes. (b) Elemental mapping images of discharged NVP electrodes. XPS spectra of (c) Na 1s, (d) Zn 2p, and (e) V 2p regions, respectively, collected at pristine, fully discharged, and fully charged states. (f) Illustration of the crystal structure and phase transition of NVP in the charged and discharged states.

516.9 eV) and V^{4+} ($2p_{3/2}$: 517.7 eV) components, following the extraction of Na ions. Only one V^{3+} signal can be observed at the pristine and discharged states, indicating good reversibility. Fig. S3 presents the survey spectra. On the basis of the above analyses, the possible electrochemical reaction mechanisms can be illustrated in Fig. 2f. Two Na ions are stripped out from NVP during the first charge process, and then, Na^+ and Zn^{2+} ions exhibit a highly reversible co-(de)intercalation reaction during the following cycles, implying that the Na/Zn-storage mechanisms of NVP in the non-aqueous and aqueous hybrid electrolytes are similar [24].

NVP has been successfully used in ZIBs; however, the fast capacity attenuation is unsatisfactory. There is an urgent need to investigate the fading mechanisms in both aqueous and non-aqueous electrolytes. Therefore, we comprehensively analyzed the structural, morphological, and composition evolutions of NVP. Fig. 3a shows the XRD patterns of NVP before and after cycling in the three kinds of electrolytes (non-aqueous Na/Zn dual-salt, non-aqueous Zn^{2+}-containing, and aqueous Na/Zn dual-salt electrolytes). Upon cycled in the aqueous electrolyte at a

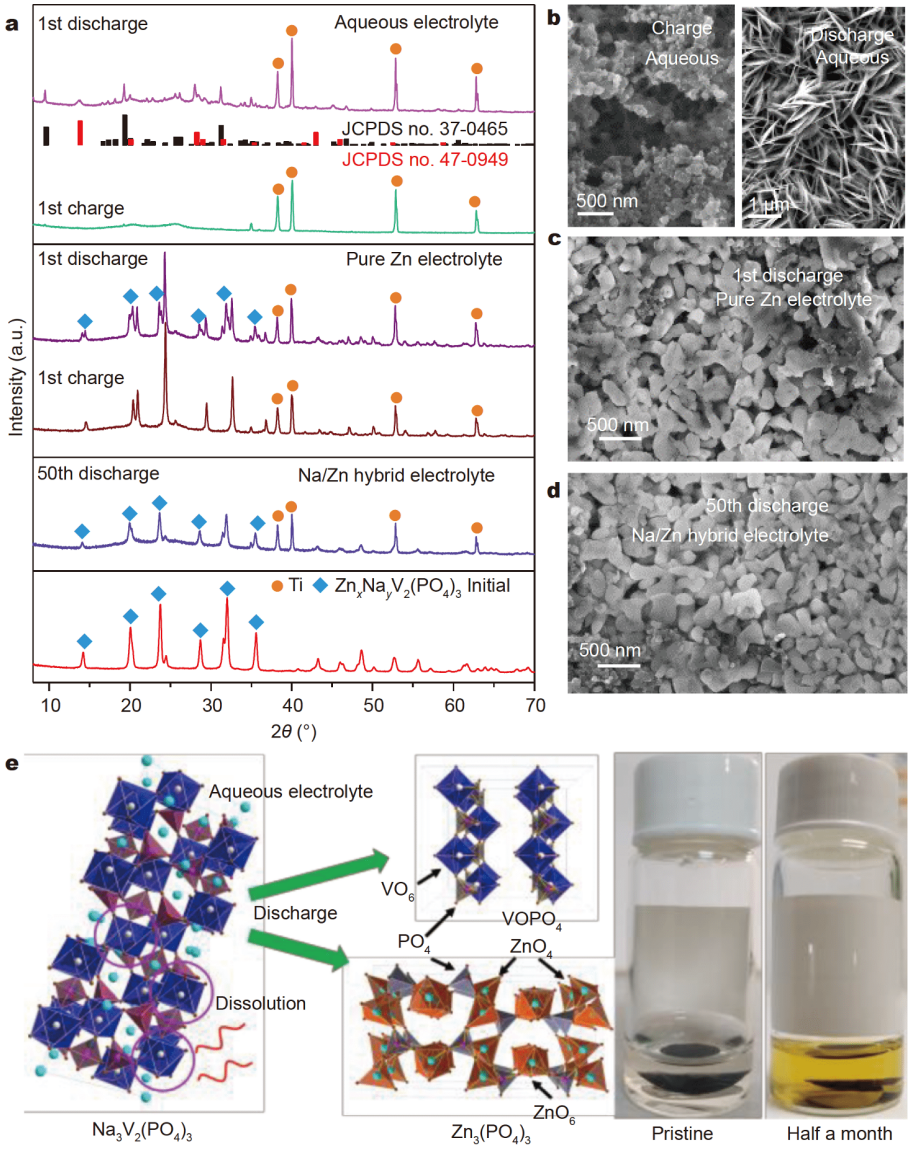

Figure 3 The capacity attenuation analysis in non-aqueous electrolytes. (a) XRD patterns of cycled NVP electrodes in different electrolytes. SEM images of NVP electrodes cycled in (b) aqueous electrolyte and (c) pure Zn^{2+}-containing electrolyte for one cycle and (d) Na/Zn hybrid electrolyte for 50 cycles. (e) Schematic illustration of the capacity attenuation mechanism of NVP and optical photographs of the NVP electrode before and after soaking in 1 mol L^{-1} $Zn(CF_3SO_3)_2$ solution for half a month.

small current of 5 mA g^{-1}, the XRD peaks of NVP disappear at fully charged states, which is also found by Zhang *at al.* [25], in which it was ascribed to the decreased crystallinity of cycled NVP. However, on the basis of Zhang's analyses [25], it cannot conclude whether the extraction of Na^+ ions or natural dissolution of NVP causes unexpected structural destruction, which will be discussed in the following. During the discharged state, we first detected the formation of the orthorhombic phase of $Zn_3(PO4)_2$ (JCPDS no. 37-0465) and the tetragonal phase of $VOPO_4$ (JCPDS no. 47-0949). The irreversible phase transition counts for the long-term cycling. When using the pure Zn^{2+}-containing electrolyte, we found that the peaks of $NaV_2(PO_4)_3$ also emerge at the discharged state, which can be explained by the incomplete intercalation of Zn and Na ions. However, good crystallinity and reversibility can still be maintained even after 50 cycles in Na/Zn dual-salt electrolyte, indicating a highly reversible reaction and robust structure, matching well with the previous study [31]. Fig. 3b exhibits the SEM

images of NVP cycled in aqueous electrolytes. At a fully charged state, the surface of NVP electrodes shows a massive, porous structure (Fig. 3b), leaving only C and F signals that can be detected by EDS tests (Fig. S4). During the long-time cycles at the small current of 5 mA g^{-1}, the pristine NVP almost disappeared. Besides, a few nanoflakes emerge on the surface of electrodes at the discharged state in aqueous electrolytes. Combining the XRD and EDS analyses, we found that the composition of those nanoflakes consists of a mixture of $Zn_3(PO4)_2$ and $VOPO_4$. The coverage of by-products on the electrode surface will undoubtedly affect the reversibility. By comparison, we found that the electrode can keep an intact shape in a non-aqueous environment even after 50 cycles (Fig. 3c, d).

According to totally different results, capacity attenuation mechanisms of NVP in aqueous and non-aqueous electrolytes might be quite defferent and need further discussion. The continuous collapse of NVP in an aqueous system will inevitably shorten the lifetime of cycling. Considering the observed phenomenon in SEM characterizations, we are inclined to believe that the dissolution of NVP triggers the severely decreasing crystallinity during charging in the aqueous electrolyte. To confirm our view, we performed a simple immersion experiment. By soaking the NVP electrodes in $Zn(CF_3SO_3)_2$, $ZnSO_4$, and $Zn(ClO_4)_2$ aqueous electrolytes (1 mol L^{-1}) for half a month, we found that the color of the solution changes from colorless to yellow, which can be explained as the dissolution of V elements, as exhibited in Fig. 3e and Fig. S5. Meanwhile, similar damages on the surface of three soaked electrodes and the decreased crystallinity match well with the charged NVP electrode results, suggesting a spontaneous dissolution phenomenon of NVP. Thus, the dissolution of NVP widely occurs in aqueous electrolytes. However, according to the XRD patterns shown in Fig. 3a, the NVP nearly disappears in the charge progress, even though the charge time (24 h) is far shorter than the soaking time. Therefore, we proposed that the spontaneous dissolution of NVP is accelerated during charging, causing substantial structural destruction. As shown in Fig. 3e, the dissolution of NVP leads to a rapid collapse of the structure, and then, during discharging, a mixture of $Zn_3(PO4)_2$ and $VOPO_4$ is irreversibly generated on the surface of the electrode, resulting in the capacity fading. It is the first time that systematic analysis and interpretation have been made on the failure mechanisms of NVP electrodes in an aqueous ZIB.

Although the non-aqueous pure Zn^{2+}-containing electrolyte avoids the dissolution of NVP in the electrolyte, poor reversibility is evidenced by the XRD patterns shown in Fig. 3a. Without the shielding effect of coordination water molecules, the strong electrostatic repulsion between inserted cations and cathode materials will hinder the intercalation reaction during discharging, resulting in low reversibility and capacity [32,33]. As shown in Fig. S6, the EDS results suggest that only a small amount of zinc elements can be detected at the discharged state even in pure Zn^{2+}-containing electrolyte, indicating a tougher intercalation process of Zn ions compared with that of Na ions. The slow extraction process during charging will also affect the reversibility, leading to capacity attenuation. Interestingly, the mole ratio of Na/Zn based on the EDS results in Figs S2 and S6 can be approximately calculated as 2.5/0.5 and 10/1 in Na/Zn dual-salt and pure Zn^{2+}-containing non-aqueous electrolytes in discharged electrodes, respectively. More Zn^{2+} ions can be inserted into NVP during discharging in the hybrid electrolyte.

On the one hand, NVP, as a kind of NASICON material, may be more suitable for Na^+ ion intercalation. On the other hand, the presence of Na^+ ions may alleviate the electrostatic repulsion upon Zn^{2+} ion intercalation and promote the intercalation progress. The results are in good agreement with the previous study [29]. By introducing Na^+ ions into the non-aqueous electrolyte, we found that the battery's cycle reversibility has been further improved. Moreover, the crystallinity and morphology of NVP are well maintained even after a long time working duration. Hence, the capacity degradation of NVP electrodes in ZIBs is well suppressed in non-aqueous Na/Zn dual-salt electrolytes.

The CV and galvanostatic charge-discharge (GCD) tests provide further evidence. The CR2032 coin-type cells were manufactured by a metallic zinc anode and NVP cathode to investigate the electrochemical performances. As shown in Fig. 4a–c and Figs S7–S9, a pair of redox peaks at 1.23/1.54 V and 1.17/1.6 V can be detected in Na/Zn dual-salt and pure Zn^{2+}-containing electrolytes in the first cycle, respectively, representing the insertion and extraction of mobile Na^+ and Zn^{2+} ions [31]. In the subsequent two cycles, the CV curves nearly overlap in hybrid electrolyte but slightly shift in pure Zn^{2+}-containing electrolyte. The initial capacities in the two electrolytes are 84 and 76 mA h g^{-1}, respectively, as revealed in the GCD profiles. The slight shifts of CV curves and lower capacity are derived from the challenging intercalation process of Zn^{2+} ions in pure Zn^{2+}-containing electrolytes.

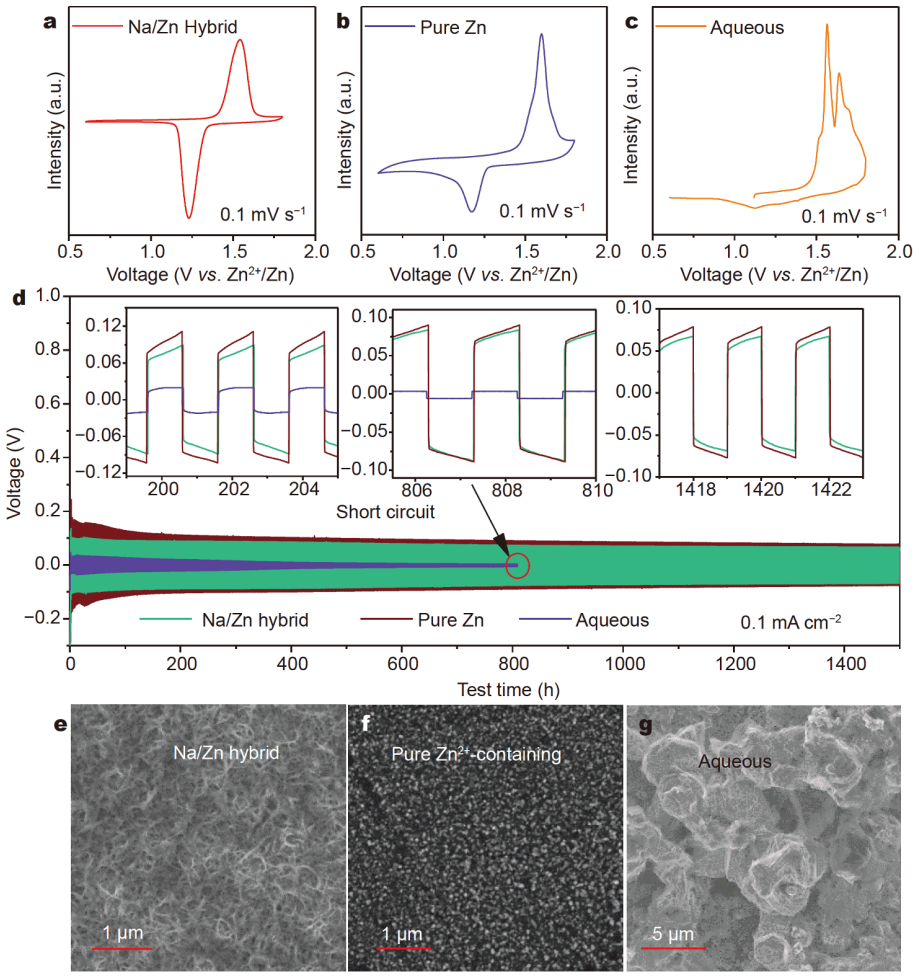

Figure 4 The long-term plating and stripping performance of zinc anode in the non-aqueous electrolyte and SEM characterization. CV tests in the first cycle: (a) Na/Zn dual-salt, (b) pure Zn^{2+}-containing, and (c) aqueous electrolytes. (d) Long-term Zn plating and stripping performances in different electrolytes and the expanded views at selected time points. SEM images of Zn anode after 150 h cycles in (e) Na/Zn dual-salt, (f) pure Zn^{2+}-containing, and (g) aqueous electrolytes.

Moreover, apart from the capacity fading when employing pure Zn^{2+}-containing electrolyte, the NVP@C electrode shows similar electrochemical behaviors in the two non-aqueous electrolytes but quite different performances in aqueous electrolytes. In the CV test, two highly irreversible oxidation peaks appear in the first scan and disappear in the next two cycles. Correspondingly, an unusual high charge capacity in the first cycle and fast capacity attenuation during subsequent cycles are manifested by GCD profiles. The abnormal anodic peaks and charge curve of the first cycle match well with the structural collapse. The different discharge curves of the first cycle may represent the formation of $Zn_3(PO_4)_2$ and $VOPO_4$. The electrochemical test results are consistent with the aforementioned capacity attenuation mechanisms for the NVP cathode.

To further evaluate the three electrolytes' practicability, we performed a long-term Zn plating and stripping test at a current density of 0.1 mA cm^{-2} by Zn/Zn symmetrical cells. After activation for approximately 200 h, the Zn electrode could be cycled with a stable overpotential in non-aqueous electrolytes (Fig. 4a). Considering the lower ionic conductivities, we found that the overpotential value of aqueous electrolytes is lower than that of non-aqueous electrolytes. However, the symmetric battery with the aqueous electrolyte suffers a short circuit after 800 h. By comparison, we found that the Zn electrodes demonstrate high stability over 1500 h in another two non-aqueous electrolytes. Fig. 4e–g exhibit the morphologies of zinc electrodes after 150 h cycles. The

deposited Zn in hybrid electrolytes manifests porous structures and is free of dendrites, which favors long-term cycling. After cycling in pure Zn^{2+}-containing electrolytes, small nanoparticles of the deposits can be seen on the zinc foil surface. In contrast, a large-size dendrite-like structure has been generated on the Zn electrode in the aqueous electrolyte, which can be attributed to the fast and uneven growth process and is apt to cause an internal short circuit (Fig. S10). The XRD test also further characterizes the formation of basic zinc salt (BZS) in the aqueous electrolyte (Fig. S11) [34,35]. During cycling, neither the Zn dendrites nor the by-products are conducive to cycle stability. No BZS was observed on the electrode surface when cycled in both two non-aqueous electrolytes.

Benefiting from the advanced non-aqueous hybrid system, NVP exhibits good electrochemical performance. As displayed in Fig. 5a, the average specific capacities of 82, 80, 77, 70, and 54 mA h g^{-1} are achieved at the current densities of 50, 100, 200, 500, and 1000 mA g^{-1}, respectively. When the current density is recovered to 50 mA g^{-1}, a highly reversible capacity of 81 mA h g^{-1} is recovered. Corresponding charge and discharge curves under various current densities are given in Fig. 5b, in which stable working voltage and charge and discharge plateaus can be observed, implying the good rate capability. When tested at a small current of 50 mA g^{-1}, the Zn/NVP battery delivers an initial capacity of 84 mA h g^{-1}. Approximately 84% capacity retention (Fig. 5c) is obtained after 200 cycles. Remarkably, the NVP electrode demonstrates a specific capacity of 74 mA h g^{-1} when measured at 500 mA g^{-1} (Fig. 5d, e). Meanwhile, 100% of the initial capacity is maintained even after 600 cycles. By comparison, we found that 39%

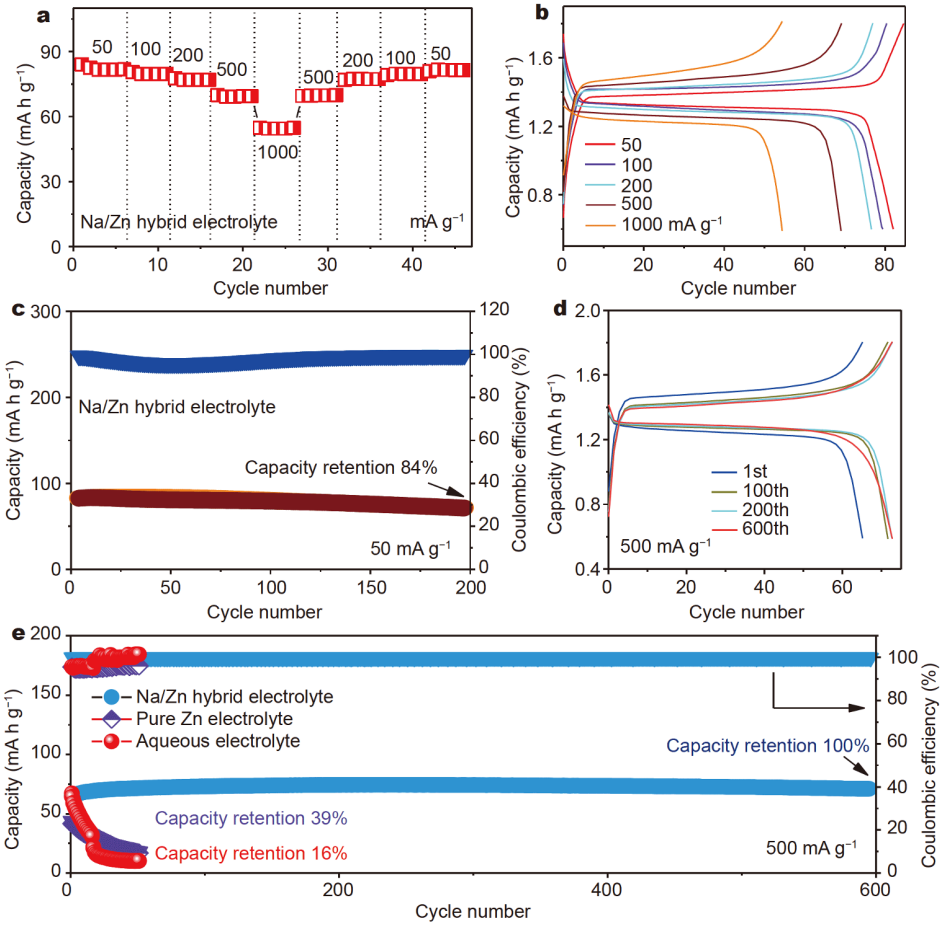

Figure 5 The electrochemical performance tests of NVP cathode in Na/Zn dual-salt electrolyte: (a) rate performance, (b) discharge and charge profiles at currents of 50, 100, 200, 500, and 1000 mA g^{-1}, (c) long-term cycling test of NVP at 100 mA g^{-1}, and (d) discharge and charge profiles at 500 mA g^{-1} for the 1st, 100th, 200th, and 600th cycles. (e) The comparison of long-term cycle performance at a current of 500 mA g^{-1} in different electrolytes.

and 16% of poor capacity retentions are obtained in pure Zn^{2+}-containing and aqueous electrolytes after merely 50 cycles, respectively. By contrast with the reported NVP cathode in ZIBs (Table S1), the non-aqueous Na/Zn dual-salt system exhibits completive advantages in specific capacities and superior performances in cycle stabilities [22–25,29]. Unfortunately, in the subsequent 600th to 800th cycles of Zn/NVP battery in the hybrid electrolyte, gradual fading of capacity, and the disappearance of charge and discharge platform can be observed in Fig. S12, suggesting the structural changes upon cycling, which may be associated with the influences of the few intercalated zinc ions, which should be studied further. We believed that proper surface engineering of NVP, allowing only Na^+ ion transport, may be an effective way to realize better cycle ability.

CONCLUSION

We first employed the NVP electrode in a non-aqueous Na/Zn dual-salt system. The co-insertion process of Na^+ and Zn^{2+} ions is validated by XRD, XPS, and EDS tests. We performed in-depth studies and analyses of capacity fading mechanisms in different electrolytes, mainly including the NVP dissolution and formation of Zn-based dendrites and by-products in aqueous electrolyte, and irreversibility of cation insertion and extraction in non-aqueous Zn^{2+}-containing electrolyte. When adopting the non-aqueous Na/Zn dual-salt electrolyte, we found that the Zn/NVP batteries demonstrate nearly 100% capacity retention after 600 cycles at 500 mA g^{-1}, which is much superior to most reported NVP-based ZIBs. This study should be useful for developing advanced cathode materials of Zn-ion batteries.

Received 28 July 2020; accepted 27 October 2020; published online 21 January 2021

1 Fang G, Zhou J, Pan A, *et al.* Recent advances in aqueous zinc-ion batteries. ACS Energy Lett, 2018, 3: 2480–2501
2 Tang B, Shan L, Liang S, *et al.* Issues and opportunities facing aqueous zinc-ion batteries. Energy Environ Sci, 2019, 12: 3288–3304
3 Wei T, Li Q, Yang G, *et al.* Pseudo-Zn-air and Zn-ion intercalation dual mechanisms to realize high-areal capacitance and long-life energy storage in aqueous Zn battery. Adv Energy Mater, 2019, 9: 1901480
4 Tang H, Peng Z, Wu L, *et al.* Vanadium-based cathode materials for rechargeable multivalent batteries: Challenges and opportunities. Electrochem Energ Rev, 2018, 1: 169–199
5 Lang J, Jiang C, Fang Y, *et al.* Room-temperature rechargeable Ca-ion based hybrid batteries with high rate capability and long-term cycling life. Adv Energy Mater, 2019, 9: 1901099
6 Shakourian-Fard M, Kamath G, Taimoory SM, *et al.* Calcium-ion batteries: Identifying ideal electrolytes for next-generation energy storage using computational analysis. J Phys Chem C, 2019, 123: 15885–15896
7 Li B, Masse R, Liu C, *et al.* Kinetic surface control for improved magnesium-electrolyte interfaces for magnesium ion batteries. Energy Storage Mater, 2019, 22: 96–104
8 Konarov A, Voronina N, Jo JH, *et al.* Present and future perspective on electrode materials for rechargeable zinc-ion batteries. ACS Energy Lett, 2018, 3: 2620–2640
9 Song M, Tan H, Chao D, *et al.* Recent advances in Zn-ion batteries. Adv Funct Mater, 2018, 28: 1802564
10 Kundu D, Adams BD, Duffort V, *et al.* A high-capacity and long-life aqueous rechargeable zinc battery using a metal oxide intercalation cathode. Nat Energy, 2016, 1: 16119
11 Yang G, Wei T, Wang C. Self-healing lamellar structure boosts highly stable zinc-storage property of bilayered vanadium oxides. ACS Appl Mater Interfaces, 2018, 10: 35079–35089
12 Hu P, Zhu T, Wang X, *et al.* Highly durable $Na_2V_6O_{16}\cdot 1.63H_2O$ nanowire cathode for aqueous zinc-ion battery. Nano Lett, 2018, 18: 1758–1763
13 Hu P, Yan M, Zhu T, *et al.* Zn/V_2O_5 aqueous hybrid-ion battery with high voltage platform and long cycle life. ACS Appl Mater Interfaces, 2017, 9: 42717–42722
14 Chen Q, Jin J, Kou Z, *et al.* Zn^{2+} pre-intercalation stabilizes the tunnel structure of MnO_2 nanowires and enables zinc-ion hybrid supercapacitor of battery-level energy density. Small, 2020, 16: 2000091
15 Ding J, Du Z, Gu L, *et al.* Ultrafast Zn^{2+} intercalation and deintercalation in vanadium dioxide. Adv Mater, 2018, 30: 1800762
16 Liao M, Wang J, Ye L, *et al.* A deep-cycle aqueous zinc-ion battery containing an oxygen-deficient vanadium oxide cathode. Angew Chem Int Ed, 2020, 59: 2273–2278
17 Liu R, Liu H, Sheng T, *et al.* Novel 3.9 V layered $Na_3V_3(PO_4)_4$ cathode material for sodium ion batteries. ACS Appl Energy Mater, 2018, 1: 3603–3606
18 Guo JZ, Wu XL, Wan F, *et al.* A superior $Na_3V_2(PO_4)_3$-based nanocomposite enhanced by both N-doped coating carbon and graphene as the cathode for sodium-ion batteries. Chem Eur J, 2015, 21: 17371–17378
19 Saravanan K, Mason CW, Rudola A, *et al.* The first report on excellent cycling stability and superior rate capability of $Na_3V_2(PO_4)_3$ for sodium ion batteries. Adv Energy Mater, 2013, 3: 444–450
20 Zhao HB, Hu CJ, Cheng HW, *et al.* Novel rechargeable $M_3V_2(PO_4)_3$//zinc (M = Li, Na) hybrid aqueous batteries with excellent cycling performance. Sci Rep, 2016, 6: 25809
21 Ming J, Guo J, Xia C, *et al.* Zinc-ion batteries: Materials, mechanisms, and applications. Mater Sci Eng-R-Rep, 2019, 135: 58–84
22 Li G, Yang Z, Jiang Y, *et al.* Towards polyvalent ion batteries: A zinc-ion battery based on NASICON structured $Na_3V_2(PO_4)_3$. Nano Energy, 2016, 25: 211–217
23 Li G, Yang Z, Jiang Y, *et al.* Hybrid aqueous battery based on $Na_3V_2(PO_4)_3$/C cathode and zinc anode for potential large-scale energy storage. J Power Sources, 2016, 308: 52–57
24 Hu P, Zhu T, Wang X, *et al.* Aqueous $Zn//Zn(CF_3SO_3)_2//Na_3V_2(PO_4)_3$ batteries with simultaneous Zn^{2+}/Na^+ intercalation/deintercalation. Nano Energy, 2019, 58: 492–498
25 Zhang X, Ma J, Hu P, *et al.* An insight into failure mechanism of NASICON-structured $Na_3V_2(PO_4)_3$ in hybrid aqueous recharge-

able battery. J Energy Chem, 2019, 32: 1–7
26 Li W, Wang K, Cheng S, *et al.* A long-life aqueous Zn-ion battery based on $Na_3V_2(PO_4)_2F_3$ cathode. Energy Storage Mater, 2018, 15: 14–21
27 Hung TF, Cheng WJ, Chang WS, *et al.* Ascorbic acid-assisted synthesis of mesoporous sodium vanadium phosphate nanoparticles with highly sp^2-coordinated carbon coatings as efficient cathode materials for rechargeable sodium-ion batteries. Chem Eur J, 2016, 22: 10620–10626
28 Duan W, Zhu Z, Li H, *et al.* $Na_3V_2(PO_4)_3$@C core–shell nanocomposites for rechargeable sodium-ion batteries. J Mater Chem A, 2014, 2: 8668–8675
29 Hu P, Zou Z, Sun X, *et al.* Uncovering the potential of M1-site-activated NASICON cathodes for Zn-ion batteries. Adv Mater, 2020, 32: 1907526
30 Jiang Y, Yang Z, Li W, *et al.* Nanoconfined carbon-coated $Na_3V_2(PO_4)_3$ particles in mesoporous carbon enabling ultralong cycle life for sodium-ion batteries. Adv Energy Mater, 2015, 5: 1402104
31 Islam S, Alfaruqi MH, Putro DY, *et al.* Pyrosynthesis of $Na_3V_2(PO_4)_3$@C cathodes for safe and low-cost aqueous hybrid batteries. ChemSusChem, 2018, 11: 2239–2247
32 Kundu D, Hosseini Vajargah S, Wan L, *et al.* Aqueous *vs.* non-aqueous Zn-ion batteries: Consequences of the desolvation penalty at the interface. Energy Environ Sci, 2018, 11: 881–892
33 Yan M, He P, Chen Y, *et al.* Water-lubricated intercalation in $V_2O_5{\cdot}nH_2O$ for high-capacity and high-rate aqueous rechargeable zinc batteries. Adv Mater, 2018, 30: 1703725
34 Li Q, Liu Y, Ma K, *et al. In situ* Ag nanoparticles reinforced pseudo-Zn-air reaction boosting $Ag_2V_4O_{11}$ as high-performance cathode material for aqueous zinc-ion batteries. Small Methods, 2019, 3: 1900637
35 Wang L, Huang KW, Chen J, *et al.* Ultralong cycle stability of aqueous zinc-ion batteries with zinc vanadium oxide cathodes. Sci Adv, 2019, 5: eaax4279

Acknowledgements This work was supported by the National Natural Science Foundation of China (91963210, U1801255, and 51872340) and the Fundamental Research Funds for the Central Universities, China (18lgpy06).

Author contributions Wang C and Yang G designed this work; Li Q synthesized the materials and carried out the electrochemical experiments; Li Q performed the *ex-situ* XRD measurements with Ma K and Hong C; Wang C, Yang G, and Li Q wrote the paper. All the authors participated in the analysis of experimental data and discussions of the results.

Conflict of interest The authors declare that they have no conflict of interest.

Supplementary information Supporting data are available in the online version of the paper.

Qian Li received his BS degree from the School of Minerals Processing and Bioengineering at Central South University in 2017. Now he is pursuing his PhD under the direction of Prof. Chengxin Wang in the School of Materials Science and Engineering at Sun Yat-sen University (SYSU). His current research focuses on rechargeable zinc-ion batteries.

Gongzheng Yang is an associate professor at the School of Materials Science and Engineering, SYSU. He received his PhD degree from SYSU in 2014. He carried out his postdoctoral research in the laboratory of Prof. Chengxin Wang in SYSU. Currently, his research interest includes energy-storage materials and devices.

Chengxin Wang is a professor in the School of Materials Science and Engineering at SYSU. Dr. Wang's research interest lies in both theoretical and experimental investigations on the nanomaterials of IV main group elements and related compounds. His current research focuses on nano energy materials.

Na/Zn双离子无水电解液抑制材料溶解及结构坍塌, 助力卓越循环能力的$Zn/Na_3V_2(PO_4)_3$电池

李乾[1], 马凯旋[1], 洪城[1], 杨功政[1*], 王成新[1,2*]

摘要 开发高性能正极材料是限制锌离子电池发展的重要因素. $Na_3V_2(PO_4)_3$ (NVP)是一种典型NASICON结构的材料, 其作为锌离子电池正极材料具有较高的工作电压, 然而其循环性能较差, 通常仅200圈. 本文首次系统地研究了该材料储锌性能的衰退机理. 研究表明, 在水系电解液中NVP的自发溶解及首圈放电过程中材料的不可逆相变是其容量衰退的主要原因. 采用含锌有机电解液虽可避免其溶解, 但锌离子的嵌入易导致晶体结构的坍塌. 本文首次引入钠离子作为新的载流子并构建有机Na/Zn混合离子电解液. 其中, 两种金属离子在NVP中高度可逆的共插层反应助力$Zn/Na_3V_2(PO_4)_3$电池实现了84 mA h g^{-1}的较高容量以及在大电流密度下循环600圈容量零衰减的高稳定性.

